Isotope effects in structural and thermodynamic properties of solid neon

Carlos P. Herrero
Instituto de Ciencia de Materiales, Consejo Superior de Investigaciones Científicas (C.S.I.C.), Campus de Cantoblanco, 28049 Madrid, Spain

(Received 17 April 2001; revised manuscript received 6 July 2001; published 12 December 2001)

Path-integral Monte Carlo simulations in the isothermal-isobaric ensemble have been carried out to study isotope effects in solid neon. This computational method allows a quantitative and nonperturbative study of these effects, which are associated with a strong anharmonicity of the atomic motion. The Ne atoms were treated as quantum particles interacting via a Lennard-Jones potential. We have studied the temperature dependence of atomic mean-square displacements, lattice parameter, bulk modulus, and heat capacity, as well as vibrational kinetic and potential energy, for the isotopes ^{20}Ne and ^{22}Ne. The studied Lennard-Jones solids are highly anharmonic, as measured from the ratio between vibrational potential and kinetic energies, which amounts to about 0.8 at 4 K. At this temperature, the isothermal bulk modulus for solid ^{22}Ne is found to be 0.3 kbar larger than that for ^{20}Ne and the cohesive energy is 32 J/mol larger for the former. The obtained heat capacity, thermal expansion, and isotopic effect in the lattice parameter agree well with experimental data.

DOI: 10.1103/PhysRevB.65.014112 PACS number(s): 67.80.−s, 05.10.Ln, 65.40.De

I. INTRODUCTION

Anharmonic effects in solids have been studied for many years, since they are responsible for important effects such as thermal expansion, pressure dependence of the compressibility, and phonon couplings, as well as the isotope dependence of structural properties and melting temperature. For solid neon, in particular, the considerable importance of such anharmonic effects has been noticed,[1,2] and the associated isotopic dependence of thermodynamic and structural properties has been found to be non-negligible.[2–6]

The lattice parameters of two chemically identical crystals with different isotopic compositions are not equal, lighter isotopes having larger vibrational amplitudes and larger lattice parameters. This effect is most noticeable at low temperatures, since the atoms in the solid feel the anharmonicity of the interatomic potential due to zero-point motion. At higher temperatures, the isotope effect on the crystal volume is less relevant and disappears in the high-temperature (classical) limit. At present, this isotopic effect in the lattice parameter of crystals can be measured with high precision.[7] Something similar happens with the compressibility, which is directly related to the anharmonicity of the solid vibrations and is expected to show a maximum isotopic effect for $T \rightarrow 0$. Other quantities, such as the vibrational energy, show an isotope dependence at low T in a harmonic approximation, due to the usual rescaling of the phonon frequencies with the isotopic mass M ($\omega \propto M^{-1/2}$), but this dependence can display appreciable changes when anharmonic effects are considered. All these effects are expected to be more important in the case of neon than for heavier rare-gas solids.[8]

From a theoretical point of view, anharmonic effects in solids have been traditionally studied by using approaches such as the so-called quasiharmonic approximation.[9,10] In this approach, frequencies of the vibrational modes in a solid are assumed to change with the crystal volume, and for given volume and temperature, the solid is supposed to be harmonic. This procedure has been employed in the last years to study isotopic effects in the crystal volume of covalent solids from *ab initio* density-functional-theory calculations.[11,12] For solid neon, in particular, isotopic differences in the zero-temperature volume and sublimation energies have been calculated for different interatomic potentials by taking into account cubic and quartic anharmonic corrections to the zero-point energy.[5] Also, the finite-temperature properties of crystalline natural Ne and ^{22}Ne were derived from a second-order self-consistent phonon theory.[6]

An alternative procedure is the Feynman path-integral (PI) method, which is a convenient theoretical approach to study anharmonic effects at temperatures at which the quantum nature of the atomic nuclei is relevant.[13,14] The combination of path integrals with Monte Carlo (MC) sampling enables us to carry out quantitative and nonperturbative studies of such anharmonic effects. The PI MC technique was applied earlier to study several properties of solid neon.[8,15] In particular, it has predicted kinetic-energy values in good agreement with the existing experimental data.[16,17] This method has been also employed to study the isotopic shift in the helium melting pressure,[18,19] as well as isotope effects in the lattice constant of solid neon[20] and diamond-type materials.[21,22] In the context of the PI formalism, several authors have developed effective (temperature-dependent) classical potentials that reproduce accurately several properties of quantum solids.[23–25] More recently, Acocella *et al.*[26] have applied an improved effective-potential Monte Carlo theory[27] to study thermal and elastic properties of solid neon.

In this paper, I present results for the lattice parameter, isothermal bulk modulus, and kinetic and potential energy, as well as atomic mean-square displacements of solid neon, as derived from PI MC simulations. These quantities are studied as functions of temperature and isotopic mass. The interatomic interaction is described by a Lennard-Jones potential.

The paper is organized as follows. In Sec. II, I describe the computational method and give some technical details. In Sec. III, I present results of the MC simulations, which are given in different subsections dealing with the energy, heat capacity, atomic mean-square displacements, lattice param-

 ©2001 The American Physical Society

eter, and bulk modulus. Finally, Sec. IV includes a discussion of the results.

II. METHOD

Equilibrium properties of solid ^{20}Ne and ^{22}Ne have been calculated by PI MC simulations in the isothermal-isobaric ensemble. Quantum exchange effects were not considered, as they are negligible for neon at the densities studied here. In the path-integral formulation of statistical mechanics, the partition function of a quantum system is evaluated through a discretization of the density matrix along cyclic paths, composed of a finite number of ''imaginary-time'' steps.[13] In the numerical simulations, this Trotter number N_T causes the appearance of N_T ''replicas'' for each quantum particle. Thus, practical implementation of this method relies on an isomorphism between the quantum system and a classical one, obtained by replacing each quantum particle (here, atomic nucleus) by a cyclic chain of N_T classical particles, connected by harmonic springs with temperature-dependent constant.[28] Details on this computational method can be found elsewhere.[29–31]

Simulations have been performed on several cubic supercells of the neon face-centered-cubic cell, with side length La, being a the unit-cell parameter and L an integer in the range from 2 to 7. Thus, the largest simulation cell considered was a $7\times7\times7$ supercell, including 1372 Ne atoms. Periodic boundary conditions were assumed. Such large supercells were necessary to study the convergence of the calculated quantities with the system size, which allowed us to extrapolate the obtained values to the infinite-size limit (see below).

The Ne atoms were treated as quantum particles interacting through a Lennard-Jones potential: $V(r)=4\epsilon[(\sigma/r)^{12}-(\sigma/r)^6]$, with $\epsilon=3.084\times10^{-3}$ eV and $\sigma=2.782$ Å. The parameter ϵ coincides with that employed in earlier PI MC simulations of liquid[32] and solid[20] Ne. However, we have taken σ to be larger than in Refs. 20 and 32 in order to reproduce the experimental lattice spacing in the limit $T\rightarrow0$. Our value for σ is close to that employed in Refs. 8, 10, and 17. The dynamic effect of the interactions between nearest neighbors is explicitly considered. The effect of interactions beyond nearest neighbors is taken into account by a static-lattice approximation.[17,20] This assumption was employed earlier in PI MC simulations of Lennard-Jones solids, giving the same results as those obtained in simulations including dynamical correlations up to several neighboring atom shells.[15] In particular, it gives good agreement with experiment for the kinetic energy of solid neon.[17] Our simulations were based on the so-called ''primitive'' form of PI MC, and the ''crude'' energy estimator was used.[28,33]

Sampling of the configuration space has been carried out by the Metropolis method[34] at temperatures between 4 and 24 K, and at a constant pressure of 1 atm. For given temperature and isotopic mass, a typical run consisted of the generation of about 10^4 paths per atom for system equilibration, followed by 5×10^5 paths per atom for the calculation of ensemble average properties. To improve the accuracy in the results for the lattice parameter, at $T>18$ K we generated 10^6 paths per atom. More details on the actual application of this method are given in Ref. 29.

In the isothermal-isobaric ensemble, the mean-square fluctuations in the volume V of the simulation cell are given by

$$(\Delta V)^2=\frac{V}{B}k_BT, \tag{1}$$

where $B=-V(\partial P/\partial V)_T$ is the isothermal bulk modulus of the solid. Hence, the fluctuations in the lattice parameter a are

$$(\Delta a)^2=\frac{k_BT}{9L^3aB}. \tag{2}$$

For a given temperature and simulation-cell size, the fluctuations $(\Delta a)^2$ can be obtained from Monte Carlo simulations. Thus, we will employ Eq. (2) to obtain the bulk modulus B from the simulation results. From Eq. (1) one can see that the relative fluctuation in the volume of the simulation cell, $\Delta V/V$, scales as $L^{-3/2}$. In fact, for ^{20}Ne at 20 K we find in the PI MC simulations, $\Delta V/V=0.023$ for $L=2$ and 6×10^{-3} for $L=5$.

Finite-size effects are expected to be observed in the structural and thermodynamic variables derived from PI MC simulations. Due to the finite dimensions of the simulation cell, long-wavelength acoustic phonons with $\lambda\gtrsim La$ (close to the center of the Brillouin zone) are truncated, introducing an artificial low-energy cutoff $\omega_0\propto1/L$ for the solid vibrations. This causes the appearance of an effective energy gap for vibrational excitations in the simulated solid that is not present in the actual material. The dependence of several equilibrium properties of rare-gas solids on the simulation-cell size has been studied in detail by Müser *et al.*[20] From this size dependence one can extrapolate the simulation results to the thermodynamic limit ($L\rightarrow\infty$). The finite-size corrections of several equilibrium properties scale as $1/V\propto L^{-3}$, as is the case of the internal energy, which converges relatively fast for our purposes.

The spatial delocalization of the neon atoms can be obtained directly from the quantum simulations and may be quantified by the mean-square displacement $(\Delta r)^2$. This magnitude, however, converges especially slowly as the cell size is increased. In Fig. 1 we present $(\Delta r)^2$ for solid Ne versus the inverse cell size. Open symbols correspond to ^{20}Ne and solid symbols to ^{22}Ne. Finite-size corrections to the atomic mean-square displacements scale linearly with $1/L$. For $L=5$ and $T=20$ K, the calculated $(\Delta r)^2$ is about 90% of the extrapolated thermodynamic limit (the error introduced by the finite cell size is $\sim10\%$). This contrasts with the convergence of the kinetic energy, which for the same L and T has an error smaller than 0.1% when compared with the corresponding extrapolated value.

For $(\Delta r)^2$ the convergence with cell size becomes slower as the temperature is raised (larger slope of the dashed lines in Fig. 1). This is a consequence of the fact that at high temperature ($k_BT>\hbar\omega$), the contribution to $(\Delta r)^2$ of a given vibrational mode with frequency ω scales as $1/\omega^2$,

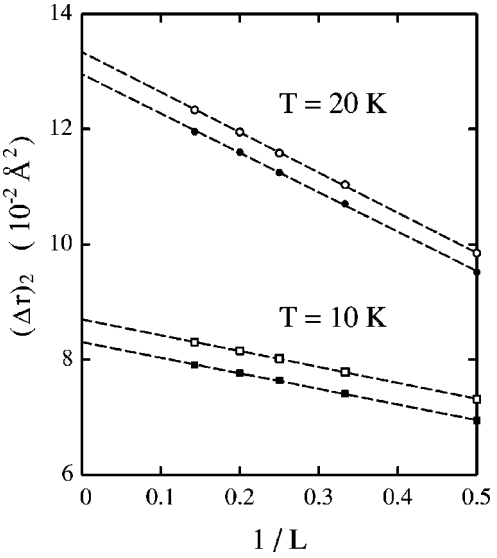

FIG. 1. Mean-square displacement, $(\Delta r)^2$, of the Ne atoms vs the inverse simulation-cell size L. Symbols represent results of PI MC simulations for isotopically pure crystals of ^{20}Ne (open symbols) and ^{22}Ne (solid symbols). Circles correspond to $T=20$ K and squares to $T=10$ K. Error bars are smaller than the symbol size. Lines are least-squares fits to the data points.

making very important the contribution of the low-energy modes neglected in the finite-size calculations. This contribution to the mean-square displacement $(\Delta r)^2$ is given approximately by[20,35]

$$(\Delta r)^2_{negl} \simeq C \int_0^{\omega_0} \rho(\omega) \frac{k_B T}{M\omega^2} d\omega, \tag{3}$$

where C is a normalization constant. Assuming a vibrational density of states $\rho(\omega) \propto \omega^2$, which is expected to be a good approximation at low frequencies (Debye model), one finds $(\Delta r)^2_{negl} \propto \omega_0 \propto 1/L$, in agreement with the results of the PI MC simulations presented in Fig. 1.

Another source of possible inaccuracies in the results obtained from PI MC simulations is the finite Trotter number N_T employed in the discretization of the path integrals. Thus, an extrapolation $N_T \to \infty$ has to be carried out to obtain precise values for the studied quantities.[20,36] Nevertheless, the convergence with N_T of the properties studied here is much faster than that described above for the simulation-cell size. For example, finite-N_T corrections to $(\Delta r)^2$ scale as $1/N_T^2$, as for the other thermodynamic and structural properties studied in Refs. 20 and 36. For a given temperature T, the largest Trotter number N_T employed in our simulations was taken as the integer number giving $N_T T \simeq 180$ K. This means that, for example, a PI MC simulation on a $5\times5\times5$ supercell ($N=500$ atoms) at 4 K ($N_T=45$) is equivalent in computational effort to a classical MC simulation of $N_T N = 22500$ atoms.

III. RESULTS

A. Energy

For given volume and temperature, the internal energy of the solid, $E(V,T)$, can be written as

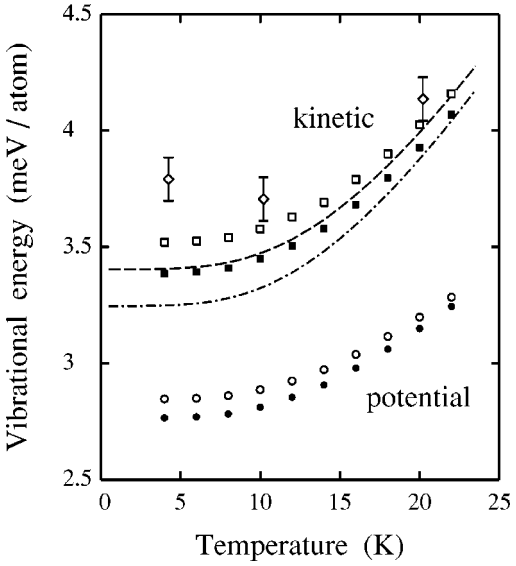

FIG. 2. Temperature dependence of the vibrational energy of solid neon. Squares and circles correspond to kinetic and potential energy, respectively, as derived from PI MC simulations. Open symbols, ^{20}Ne; solid symbols, ^{22}Ne. Error bars of the simulation results are less than the symbol size. The dashed and dash-dotted lines correspond to a Debye model for ^{20}Ne and ^{22}Ne, respectively, with $\Theta_D(^{20}\text{Ne})=70$ K. Diamonds are results for the kinetic energy of ^{20}Ne, obtained by Timms *et al.* (Ref. 16) from inelastic neutron scattering in solid neon with natural isotopic composition.

$$E(V,T) = E_0 + E_S(V) + E_{vib}(V,T), \tag{4}$$

where E_0 is the minimum potential energy for the (classical) crystal at $T=0$ K, $E_S(V)$ is the elastic energy, and $E_{vib}(V,T)$ is the vibrational energy. With the parameters employed here for the Lennard-Jones potential, we find $E_0 = -26.55$ meV per neon atom, which corresponds to a (classical) lattice parameter $a_{cl}(0)=4.2890$ Å. This value for E_0 translates into a cohesive energy of 2.57 kJ/mol.

For a given volume V, the classical energy at $T=0$ (point atoms on their lattice sites) increases by an amount $E_S(V)$ with respect to the minimum energy E_0. This elastic energy E_S depends only on the volume, but at finite temperatures and for the real (quantum) solid, it depends implicitly on T due to the temperature dependence of V (thermal expansion). The elastic energy $E_S(V)$ represents a non-negligible part of the internal energy and for ^{20}Ne is found to be 1.21 and 2.14 meV per atom at 4 and 24 K, respectively. Note that the elastic energy at 4 K is basically due to the change in volume caused by ''zero-point'' lattice expansion.

The vibrational energy $E_{vib}(V,T)$ depends explicitly on both V and T and can be obtained by subtracting the elastic energy from the internal energy. Path-integral Monte Carlo simulations allow us to obtain separately the kinetic E_k and potential energy E_p associated with the lattice vibrations, as a function of temperature.[30] Both energies are shown in Fig. 2 for ^{20}Ne (open symbols) and ^{22}Ne (solid symbols). Squares and circles correspond to the vibrational kinetic and potential energy, respectively. Our results for the kinetic energy are close to those derived earlier from PI MC simula-

tions with Lennard-Jones[8,16,17] and Aziz[16] interatomic potentials. For comparison, we present values of the kinetic energy of ^{20}Ne, derived by Timms *et al.*[16] from inelastic neutron scattering in solid neon with natural isotopic composition (diamonds).[37] The kinetic energy of ^{21}Ne (natural abundance 0.27%) in solid neon has been more recently measured by using resonant nuclear reactions,[38] and a value of 3.2 (± 0.6) meV/atom was found at $T=8$ K (not shown in the figure for the sake of clarity). The results of our PI MC simulations indicate that the vibrational potential energy is clearly smaller than the kinetic energy, for both solid ^{20}Ne and ^{22}Ne. As a result, E_p is about 20% lower than E_k in the whole temperature range under consideration.

For comparison, we also present in Fig. 2 the kinetic and potential energy obtained for ^{20}Ne and ^{22}Ne from a Debye model for the lattice vibrations (dashed and dash-dotted lines, respectively). In this approximation, the kinetic (potential) energy per atom at temperature T is given by

$$E_k^D = E_p^D = \frac{9}{4}\frac{\hbar}{\omega_D^3}\int_0^{\omega_D} \omega^3 \coth\left(\frac{1}{2}\beta\hbar\omega\right) d\omega, \qquad (5)$$

where $\beta = 1/(k_B T)$ and ω_D is the Debye frequency (see, e.g., Ref. 38 for an equivalent expression for E_k^D). For ^{20}Ne we have taken $\omega_D(^{20}\text{Ne}) = 48.7$ cm^{-1}, which corresponds to a Debye temperature $\Theta_D = 70$ K.[39] The Debye frequency is assumed to scale with the isotopic mass M as $\omega_D \propto M^{-1/2}$, and thus we have taken $\omega_D(^{22}\text{Ne}) = 46.4$ cm^{-1}. The kinetic energy derived from the PI MC simulations is higher than that found from this Debye approximation, but the potential energy obtained in the simulations is clearly lower for both neon isotopes.

A quantitative evaluation of the overall anharmonicity of the atom vibrations can be obtained from the PI MC simulations by calculating the ratio between potential and kinetic energy at different temperatures. This ratio should be 1 for a harmonic solid at any temperature, as follows from the virial theorem. In Fig. 3 we display the temperature dependence of the potential-to-kinetic energy ratio for ^{20}Ne (squares) and ^{22}Ne (circles), derived from our quantum simulations. This ratio is found to be of the order of 0.8 for both isotopes, showing a clear departure from the harmonic expectancy. It decreases as temperature rises and is higher for ^{22}Ne than for ^{20}Ne, as expected from the fact that the heavier isotope should be closer to the classical limit, for which one has, at $T=0$, $E_p/E_k = 1$.

The departure from harmonicity of the solid vibrations can be also analyzed by studying the ratio between kinetic or potential energies of both neon isotopes, ^{20}Ne and ^{22}Ne. This is shown in Fig. 4, where we present the temperature dependence for the ratio $E_p(^{22}\text{Ne})/E_p(^{20}\text{Ne})$ between potential energies (circles) and for the ratio $E_k(^{22}\text{Ne})/E_k(^{20}\text{Ne})$ between kinetic energies of both isotopes (squares). The dashed line corresponds to the Debye model discussed above, which at $T=0$ converges to the value $\sqrt{20/22} = 0.953$ expected in a harmonic approximation. Both potential and kinetic energy ratios derived from the PI MC simulations are larger than the Debye harmonic approximation in the whole temperature range considered. The anharmonicity of the vibrational modes affects the potential energy more strongly than the kinetic energy of the neon atoms. The actual trend of the Debye curve in Fig. 4 can be changed by modifying the Debye temperature Θ_D, and thus this curve could approach the PI MC results (e.g., by taking smaller values for Θ_D). However, the low-temperature limit of the energy ratio pre-

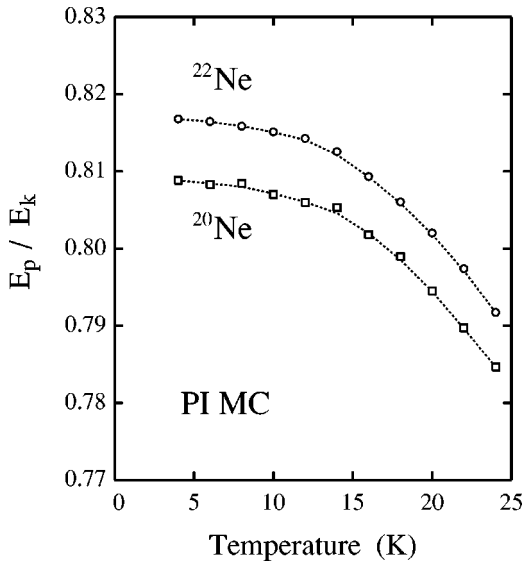

FIG. 3. Potential-to-kinetic energy ratio E_p/E_k for solid ^{20}Ne (squares) and ^{22}Ne (circles), as derived from PI MC simulations. Error bars are on the order of the symbol size. Dotted lines are guides to the eye.

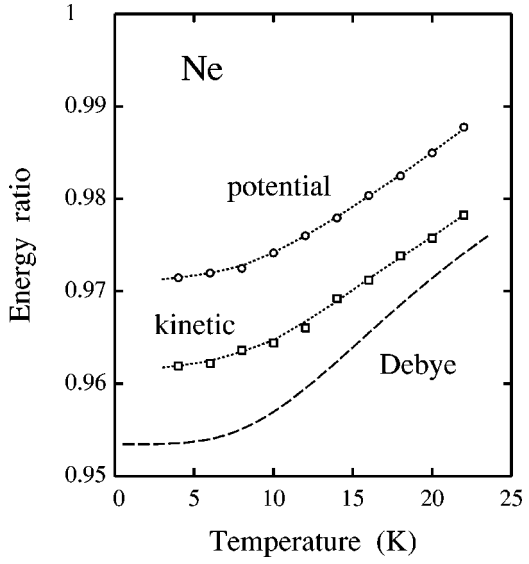

FIG. 4. Energy ratio between solid ^{22}Ne and ^{20}Ne. Circles correspond to the ratio between vibrational potential energies, $E_p(^{22}\text{Ne})/E_p(^{20}\text{Ne})$, and squares to the ratio between kinetic energies, $E_k(^{22}\text{Ne})/E_k(^{20}\text{Ne})$. Error bars are on the order of the symbol size. Dotted lines on the simulation data are guides to the eye. The dashed line is the ratio obtained for both kinetic and potential energies in a Debye model with $\Theta_D(^{20}\text{Ne}) = 70$ K and $\Theta_D(^{22}\text{Ne}) = 66.7$ K.

sented in this figure is independent of Θ_D, and the different values obtained from PI MC simulations for the ratios of kinetic and potential energies at low T actually reflect the anharmonicity of the zero-point vibrations in the crystal.

Summarizing our energy results, we find that the cohesive energy for ^{20}Ne at 4 K amounts to 18.98 meV/atom, which means an important decrease of 7.57 meV/atom with respect to the classical result at $T=0$. According to Eq. (4), this change in internal energy of the solid can be split into three contributions: elastic energy originating from lattice expansion (1.21 meV/atom) and kinetic and potential vibrational energies (3.51 and 2.85 meV/atom, respectively). For solid ^{22}Ne we find at 4 K a cohesive energy of 19.31 meV/atom, i.e., 0.33 meV/atom higher (more stable) than for solid ^{20}Ne (a difference of about 2%). At 24 K, the cohesive energy decreases to 16.75 and 16.96 meV/atom for ^{20}Ne and ^{22}Ne, respectively. Our result for the cohesive energy of ^{20}Ne at $T=0$ is about 1 meV/atom lower than that found by Acocella *et al.* from an improved effective-potential theory.[26] This difference seems to be due to the different potential parameters (and not to the different computational procedures) employed in both calculations.

B. Heat capacity

The heat capacity C_P for ^{20}Ne and ^{22}Ne has been calculated from the MC simulations at $P=1$ atm as a numerical derivative of the enthalpy, $H=E+PV$, with respect to the temperature. Our results for ^{20}Ne are shown in Fig. 5(a) as open squares. The data points found for ^{22}Ne lie slightly higher than those corresponding to ^{20}Ne and are not shown for the sake of clarity. In this figure we also present the experimental results obtained by Somoza and Fenichel[4] for ^{20}Ne (solid line), as well as those found by Fenichel and Serin[40] for natural neon (dashed line). Taking into account the average isotopic mass of natural neon ($M_{av}=20.18$ amu), the latter results should be slightly higher than the former, contrary to the trend observed in the data actually measured, indicating that the difference between both sets of data at $T>16$ K is caused by experimental uncertainty. This is in line with the indications by Somoza and Fenichel,[4] in the sense that at $T\gtrsim 18$ K the error introduced by uncertainties in the temperature and to the partial vaporization of the solid increases appreciably. Our results follow closely the experimental data up to $T=18$ K, and at $T\geqslant 18$ K they seem to be slightly lower.

In Fig. 5(b) we present the relative change in heat capacity, $\psi=(C_P^{22}-C_P^{20})/C_P^{20}$, as a function of temperature. The PI MC results are shown as open squares, and the solid line represents the data obtained by Somoza and Fenichel.[4] Our results follow closely the experimental data at $T>8$ K. At lower T, the error in the ψ values derived from the simulations increases very fast as C_P approaches zero. An arrow in Fig. 5(b) indicates the zero-temperature value expected for ψ in a Debye (harmonic) approximation, irrespective of the assumed Debye temperature. In fact, at $T\ll\Theta_D$, $C_P\propto(T/\Theta_D)^3$, whence we have $C_P\propto T^3M^{3/2}$, and $\psi\rightarrow 0.154$ at low T in this approximation. Values of ψ derived from experiment at $T<6$ K decrease as the temperature is lowered, contrary to the expectancy of any harmonic model for the lattice vibrations.

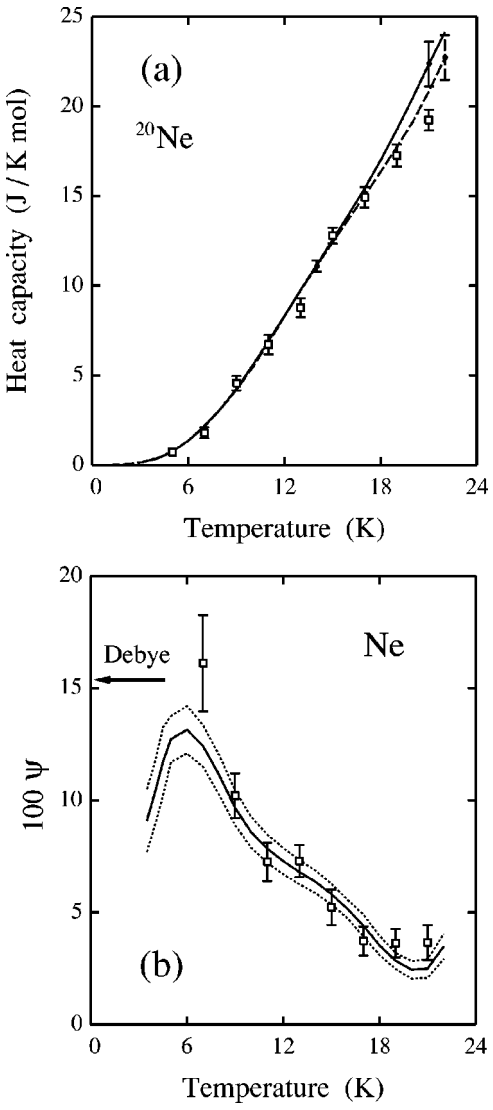

FIG. 5. (a) Heat capacity C_P of solid neon as a function of temperature. Squares indicate results of PI MC simulations for ^{20}Ne. The solid and dashed lines are experimental results for solid ^{20}Ne (Ref. 4) and for solid neon with natural isotopic composition (Ref. 40), respectively. Error bars are given for three experimental points, indicated by black dots. (b) Relative change in heat capacity, $\psi=(C_P^{22}-C_P^{20})/C_P^{20}$, vs temperature. Symbols represent results of our PI MC simulations, and the solid line indicates the experimental data from Somoza and Fenichel (Ref. 4). Two dotted lines above and below the experimental results correspond to the error bars of these data. An arrow shows the value of ψ obtained in a Debye model at $T=0$ K.

C. Atomic mean-square displacements

The mean-square displacements $(\Delta r)^2$ of the neon atoms are displayed in Fig. 6(a) for temperatures between 4 and 22 K. In this figure, symbols are data points obtained from our PI MC simulations: squares, ^{20}Ne; circles, ^{22}Ne. At low tem-

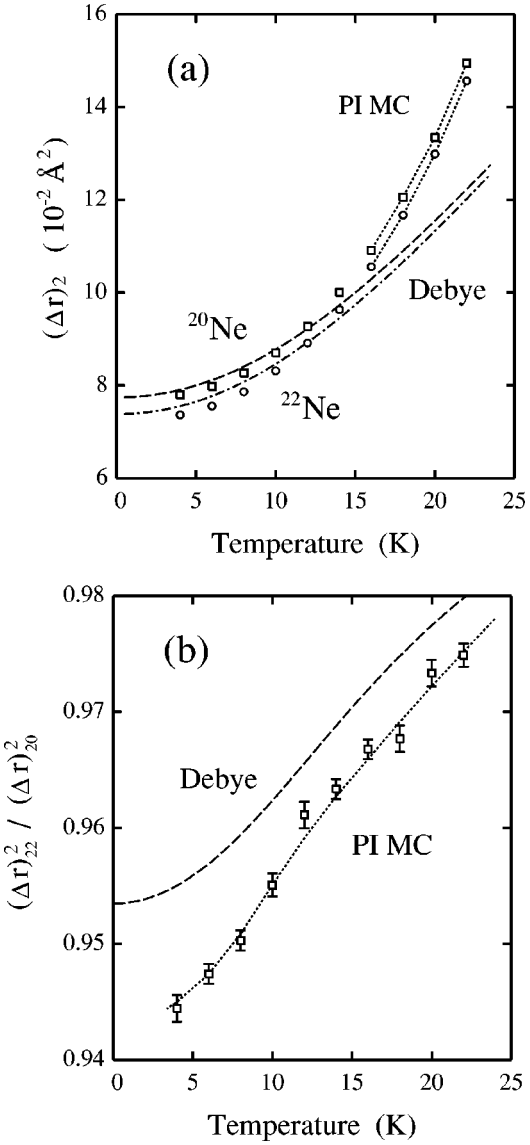

FIG. 6. (a) Temperature dependence of the mean-square displacement, $(\Delta r)^2$, for ^{20}Ne (squares) and ^{22}Ne (circles), as derived from PI MC simulations. Error bars are less than the symbol size. Dashed and dash-dotted lines: Debye model for solid ^{20}Ne and ^{22}Ne, respectively, with $\Theta_D(^{20}\mathrm{Ne})=70$ K. (b) Ratio between mean-square displacements of ^{22}Ne and ^{20}Ne: symbols, results of the PI MC simulations; dashed line, Debye model. Dotted lines in (a) and (b) are guides to the eye.

peratures, $(\Delta r)^2$ goes to the value corresponding to the zero-point motion of the atoms in the crystal, and we find $(\Delta r)^2_0$ values between 7 and 8×10^{-2} Å^2. The atomic mean-square displacements change with the isotopic mass M, isotopes with larger mass having a lower spatial delocalization. This mass dependence is most important at low temperatures and decreases as the temperature goes up. In the case of neon, $(\Delta r)^2$ for ^{20}Ne is still clearly larger than that for ^{22}Ne at temperatures close to the melting temperature, since T_m ($=24.5$ K for natural Ne) is much lower than the Debye temperature of the solid ($\Theta_D\sim70$ K). For comparison, we also present in this figure the atomic mean-square displacement obtained from a Debye model for the lattice vibrations. In this approximation, the atomic spatial delocalization at temperature T is given by[22]

$$(\Delta r)^2_D=\frac{9}{2}\frac{\hbar}{M\omega_D^3}\int_0^{\omega_D}\omega\coth\left(\frac{1}{2}\beta\hbar\omega\right)d\omega. \qquad (6)$$

With $\Theta_D(^{20}\mathrm{Ne})=70$ K, we find for ^{20}Ne and ^{22}Ne the dashed and dash-dotted lines shown in Fig. 6(a), respectively. At temperatures $T<10$ K this approach gives values for $(\Delta r)^2$ slightly larger than our PI MC results, but the simulation data become higher as temperature rises.

In Fig. 6(b) we display the ratio between mean-square displacements $(\Delta r)^2$ for isotopically pure crystals of ^{22}Ne and ^{20}Ne (squares). For comparison, we also present in this figure the delocalization ratio obtained from a Debye model for the lattice vibrations (dashed line). This approach gives results that deviate appreciably from those yielded by the MC simulations, indicating a strong effect of the anharmonicity of the vibrational modes. In fact, such a simple harmonic approach gives for the delocalization ratio results very close to those found from MC simulations in covalent solids,[22] where the anharmonicity is much smaller than in the present case. At low temperatures, the delocalization ratio obtained in the Debye model for solid Ne converges to $\sqrt{20/22}$, the expected value in a harmonic model at $T=0$. The low-temperature limit for the results of our PI MC simulations is clearly lower than the harmonic expectation. As the temperature rises, this ratio increases and should approach 1 at temperatures $T>\Theta_D$.

D. Lattice parameter

The effect of anharmonicity appears clearly in the average Ne-Ne distance (or in the lattice parameter) at low temperature, which is larger than that corresponding to the minimum potential energy of the (classical) crystal.[20] Results for the lattice parameter derived from our PI MC simulations follow closely the experimental data for ^{20}Ne and ^{22}Ne up to 24 K, as displayed in Fig. 7(a). Classical MC simulations give a nearly linear temperature dependence for the interatomic distance,[20] which converges at low T to the value corresponding to the minimum potential energy of the crystal [here, $d_{cl}(0)=3.0328$ Å]. The increase in ^{20}Ne-^{20}Ne distance obtained in the quantum simulations, with respect to that found in the classical ones at low temperature, amounts to 0.1237 Å. This quantum effect on the nearest-neighbor atom distance at $T=0$ corresponds to an increase in lattice parameter of 0.1749 Å. (Note that for a face-centered-cubic lattice $a=\sqrt{2}d$). In fact, we find for the quantum crystal a zero-temperature lattice parameter $a_{20}(0)=4.4639(2)$ Å vs $a_{cl}(0)=4.2890$ Å for the classical one. This means an increase of 4.1% in the lattice constant a due to anharmonicity of the zero-point atomic motion, which amounts to about twice the change in a due to thermal expansion between 0 K and the melting temperature of neon.

The relative change in lattice parameter between neon crystals with different isotopic composition can be measured by the quantity $\chi=(a_{20}-a_{22})/a_{22}$, which is shown in Fig.

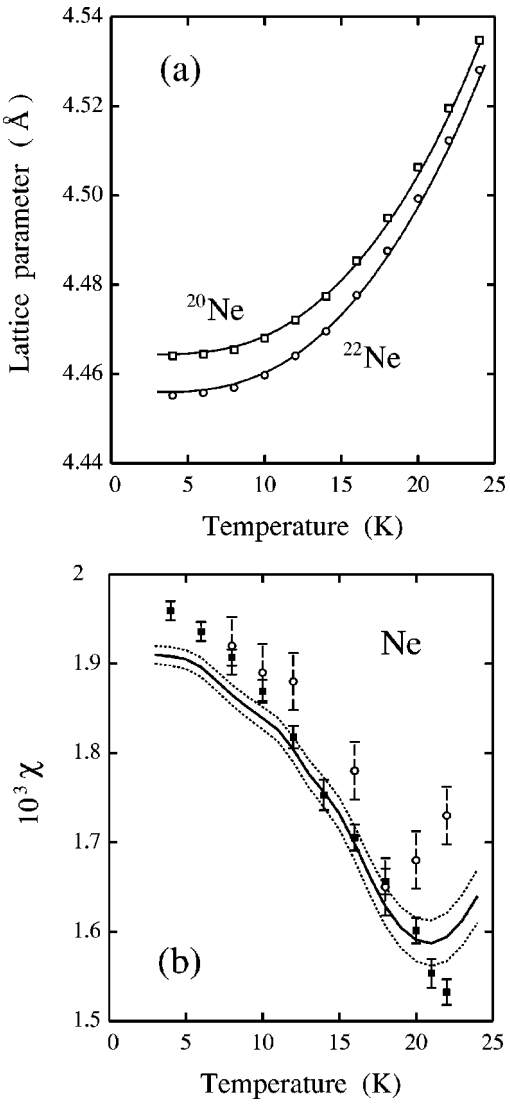

FIG. 7. (a) Temperature dependence of the lattice parameter of isotopically pure crystals of solid Ne. Squares ^{20}Ne; circles, ^{22}Ne. Error bars are less than the symbol size. Solid lines represent results derived from x-ray diffraction experiments by Batchelder *et al.* (Ref. 3). Error bars of the experimental data are less than the linewidth. (b) Relative change in the lattice parameter, $\chi=(a_{20}-a_{22})/a_{22}$, vs the temperature. Solid squares, results of the present PI MC simulations; open circles, results from Müser *et al.* (Ref. 20); solid line, experimental data from Ref. 3. Two dotted lines above and below the experimental results correspond to the error bars of these data.

7(b). Solid squares indicate results of the present PI MC simulations, which are compared with those obtained from x-ray diffraction experiments[3] (solid line). We also present results derived from PI MC simulations by Müser *et al.*[20] (open circles). For increasing temperature, the relative change χ decreases, since quantum effects become less relevant to describe the atomic motion. However, the experimental data show an increase in χ at temperatures higher than 20 K, close to the melting temperature of neon. Our results do not reproduce this increase in χ, which was apparently obtained in the PI MC simulations of Ref. 20 [see open

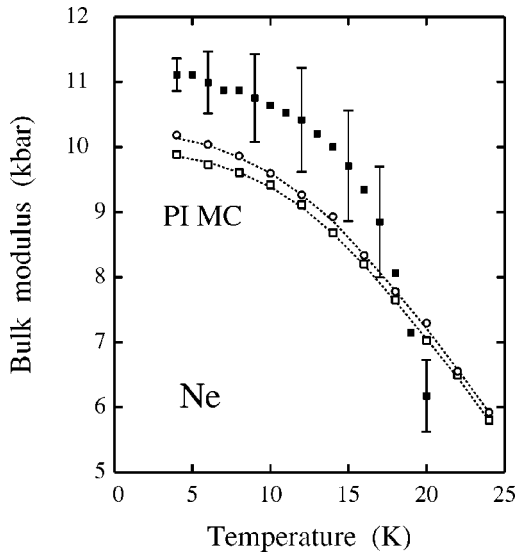

FIG. 8. Isothermal bulk modulus as a function of temperature. Open symbols represent results of PI MC simulations: Squares for ^{20}Ne and circles for ^{22}Ne. Error bars are of the order of the symbol size. Dotted lines are guides to the eye. Solid squares indicate experimental results from Batchelder *et al.* (Ref. 42).

circles in Fig. 7(b)]. We have carried out some simulations with the same potential parameters and cutoff distance for dynamic correlations employed in Ref. 20 (up to the fourth neighboring shell), but did not find such an increase in χ at $T>20$ K. A possible explanation for this increase in isotopic effect in the experimental data is related to the generation of thermal equilibrium vacancies,[3] which are not allowed in our MC simulations. Moreover, the experimental data at $T>18$ K could be affected by the problems discussed above in connection with the heat capacity results (partial vaporization of the solid and temperature uncertainties).

The temperature dependence of the lattice constant of natural neon and ^{22}Ne was calculated by Goldman *et al.*[6] from a self-consistent phonon theory. These authors found for a 6-12 Lennard-Jones potential at $T=0$ a relative isotopic difference $\chi(0)=2.0\times10^{-3}$, close to the extrapolation of experimental data[3] [$\chi_{\text{expt}}(0)=1.91\times10^{-3}$] and to our low-temperature results. This method gave a values differing from experiment by 1.4×10^{-3} Å at $T=0$, to be compared with a difference of 5×10^{-4} Å found for our simulation results. This difference with experiment increases as temperature is raised, and at 18 K, we found 1.3×10^{-3} Å vs $\sim3\times10^{-3}$ Å for the results in Ref. 6.

E. Bulk modulus

The isothermal bulk modulus of solid neon has been calculated from the mean-square fluctuations of the lattice parameter by using Eq. (2). The results are plotted in Fig. 8, where squares and circles correspond to ^{20}Ne and ^{22}Ne, respectively. At 4 K we find $B=9.88(3)$ kbar for ^{20}Ne and 10.19(3) kbar for ^{22}Ne. These values are very close to those found by Goldman *et al.*[6] from their self-consistent phonon theory at $T=0$: $B=9.94$ and 10.22 kbar, respectively. Thus, we find a difference of 0.31 kbar between both isotopes (a

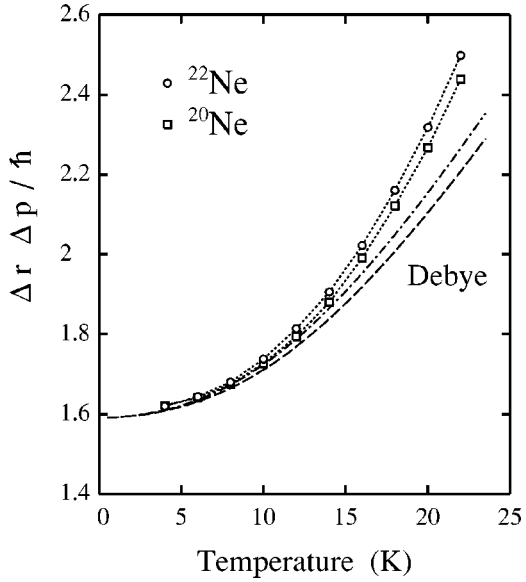

FIG. 9. Temperature dependence of the product $\Delta r \Delta p$ for solid neon. Symbols indicate results of PI MC simulations: squares for ^{20}Ne and circles for ^{22}Ne. Dotted lines are guides to the eye. The dashed and dash-dotted lines were derived from a Debye model for the lattice vibrations with $\Theta_D(^{20}\mathrm{Ne}) = 70$ K and $\Theta_D(^{22}\mathrm{Ne}) = 66.7$ K.

3% of the calculated values). This difference is reduced to ~ 0.1 kbar at 24 K. We note that the classical expectancy (which in our context corresponds to the limit $M \to \infty$) at $T = 0$ is $B_{cl}(0) = 75\epsilon/\sigma^3 = 17.2$ kbar (see, e.g., Ref. 41). This means that quantum effects cause an important decrease in B, which for ^{20}Ne amounts to 42% of the classical value at $T \to 0$.

Experimental results for natural neon obtained by Batchelder *et al.*[42] are displayed in Fig. 8 as solid symbols. At low temperatures ($T < 18$ K) these data are larger than our PI MC results, and at higher T, the experimental data decrease faster than those derived from the simulations. Our results for the bulk modulus of solid neon are very close to those found by Acocella *et al.*[26] by using an improved effective-potential Monte Carlo theory with Lennard-Jones and Tang-Toennis-type[43] interatomic potentials. This method gives results for the lattice parameter a and heat capacity C_V in good agreement with experimental data, but similarly to our PI MC simulations, predict values for the bulk modulus B lower than the experimental findings at $T < 18$ K. Thus, interatomic potentials that reproduce well several structural and thermodynamic properties of solid neon give too small values for the low-temperature bulk modulus.

IV. DISCUSSION

From the results of the quantum simulations presented above, one can study the delocalization of the atomic nuclei in phase space as a function of temperature. With this purpose, we calculate the product $\Delta r \Delta p$ between the root-mean-square fluctuations of the position and momentum of the neon atoms. The latter are related to the kinetic energy by the relation $(\Delta p)^2 = 2ME_k$. In Fig. 9 we present the product $\Delta r \Delta p$ as a function of temperature for ^{20}Ne (squares) and ^{22}Ne (circles), as derived from the PI MC simulations. The dashed and dash-dotted lines correspond to the Debye model discussed above for ^{20}Ne and ^{22}Ne, respectively. In this approximation, the product $\Delta r \Delta p$ at $T = 0$ amounts to $1.59\hbar$, irrespective of ω_D. Note that for an isotropic three-dimensional (3D) harmonic oscillator this product takes at $T = 0$ the value $3\hbar/2$. At $T = 4$ K, we find, for both ^{20}Ne and ^{22}Ne, $\Delta r \Delta p = 1.62\hbar$, very close to the value expected in a Debye model. Differences between both neon isotopes in the product $\Delta r \Delta p$ increase as temperature rises, $\Delta r \Delta p$ being larger for ^{22}Ne. In fact, in a Debye model, at high temperatures ($k_B T > \hbar\omega_D$) one has $\Delta r \Delta p = 3\sqrt{3} k_B T/\omega_D$, and hence $\Delta r \Delta p \propto TM^{1/2}$.

In the presentation of our simulation results, we have compared the MC data with those predicted by a Debye model with a constant (temperature-independent) Θ_D. The main purpose of this comparison was to assess the importance of anharmonic affects in the various quantities considered. Usually, Θ_D is assumed to change with temperature, in order to fit experimental heat capacity data. Something similar could be done with our simulation results, by assuming a temperature-dependent $\Theta_D(T)$. For example, one could fit the MC data for the kinetic energy E_k presented in Fig. 2 by increasing Θ_D. However, this *ad hoc* fit would not match the potential energy, which is clearly smaller than E_k (an anharmonic effect that cannot be taken into account by changing Θ_D). Also, to fit other quantities, a different function $\Theta_D(T)$ is necessary, as is the case of $(\Delta r)^2$, for which Θ_D should be at $T > 12$ K lower than the value employed above to calculate the lines shown in Fig. 6(a).

Anharmonic effects in solid Ar have been quantified earlier by comparing the kinetic and potential energies derived from PI MC simulations.[20] In the limit $T \to 0$ the potential energy was found to be 7% lower than the kinetic energy, indicating an important anharmonicity of the zero-point motion in this solid. Such an anharmonicity is expected to be larger for Ne. In fact, from the results shown in Fig. 3, we find that at low temperatures E_p is 19% and 18% lower than E_k for ^{20}Ne and ^{22}Ne, respectively. These values are very large when compared with those found for covalent solids at low temperatures. For example, for diamond, silicon, and germanium one finds at low T differences between E_p and E_k smaller than 1%, and at the Debye temperature of each material, they are less than 3%.[21,22,44] Another interesting point is that for these covalent materials the vibrational E_p is larger than E_k, just the opposite to the trend found for rare-gas solids. Thus, the fact that $E_p < E_k$, found for Ne and Ar, is not general in solids and can be associated with the particular character of the interatomic interactions present in rare-gas (Lennard-Jones) solids.

The low-temperature changes in the lattice parameter a due to isotopic mass can be explained quantitatively from the zero-point lattice expansion $a_{\mathrm{ref}}(0) - a_{cl}(0)$ for a crystal with a reference isotopic mass M_{ref}. In fact, in a quasiharmonic approach the difference $\Delta a(0) \equiv a_M(0) - a_{\mathrm{ref}}(0)$ at $T = 0$ can be expressed as[22,45]

$$\Delta a(0) = [a_{\mathrm{ref}}(0) - a_{cl}(0)](\sqrt{M_{\mathrm{ref}}/M} - 1). \quad (7)$$

Taking ^{20}Ne as our reference, we have $a_{20}(0) - a_{cl}(0) = 0.1749$ Å (see above), and for the isotopic difference $a_{22}(0) - a_{20}(0)$, Eq. (7) gives $\Delta a(0) = -8.1 \times 10^{-3}$ Å. This value is close to the low-temperature results found from direct calculation of the lattice parameters corresponding to different atomic masses [squares and circles in Fig. 7(a)].

In summary, we have studied the dependence of structural and thermodynamic properties of solid neon on isotopic mass by path-integral Monte Carlo simulations. These quantum simulations allow us to study phonon-related properties of solids, without the assumption of a harmonic or quasiharmonic approximation, usually employed in theoretical studies. In this way, we could separate the kinetic and potential contributions to the vibrational energy of the solid and found that their relative values depart appreciably from those expected in harmonic approaches. We have found quantitative agreement with experimental data for the isotope effect in the heat capacity C_P and lattice parameter. The calculated isothermal bulk modulus is smaller than the experimental data at low temperatures, but the relative difference of 3% between $B(^{22}\mathrm{Ne})$ and $B(^{20}\mathrm{Ne})$ is expected to be close to the actual one. More experimental and theoretical work will be necessary to understand the difference between calculated and experimental results for the bulk modulus of solid neon.

ACKNOWLEDGMENTS

The author benefited from discussions with R. Ramírez, T. López-Ciudad, and L. M. Sesé. This work was supported by CICYT (Spain) through Grant No. BFM2000-1318 and by DGESIC through Project No. 1FD97-1358.

[1] H.D. Jones, Phys. Rev. Lett. **23**, 766 (1969).
[2] R.M. Kimber and S.J. Rogers, J. Phys. C **6**, 2279 (1973).
[3] D.N. Batchelder, D.L. Losee, and R.O. Simmons, Phys. Rev. **173**, 873 (1968).
[4] E. Somoza and H. Fenichel, Phys. Rev. B **3**, 3434 (1971).
[5] J.S. Brown and J.L. Feldman, Proc. Phys. Soc. London **89**, 993 (1966).
[6] V.V. Goldman, G.K. Horton, and M.L. Klein, J. Low Temp. Phys. **1**, 391 (1969).
[7] A. Kazimorov, J. Zegenhagen, and M. Cardona, Science **282**, 930 (1998).
[8] A. Cuccoli, A. Macchi, V. Tognetti, and R. Vaia, Phys. Rev. B **47**, 14 923 (1993).
[9] G.P. Srivastava, *The Physics of Phonons* (Adam Hilger, Bristol, 1990).
[10] R.G. Della Valle and E. Venuti, Phys. Rev. B **58**, 206 (1998).
[11] P. Pavone and S. Baroni, Solid State Commun. **90**, 295 (1994).
[12] S. Biernacki and M. Scheffler, J. Phys.: Condens. Matter **6**, 4879 (1994).
[13] R.P. Feynman, *Statistical Mechanics* (Addison-Wesley, New York, 1972).
[14] H. Kleinert, *Path Integrals in Quantum Mechanics, Statistics and Polymer Physics* (World Scientific, Singapore, 1990).
[15] M. Neumann and M. Zoppi, Phys. Rev. B **62**, 41 (2000).
[16] D.N. Timms, A.C. Evans, M. Boninsegni, D.M. Ceperley, J. Mayers, and R.O. Simmons, J. Phys.: Condens. Matter **8**, 6665 (1996).
[17] A. Cuccoli, A. Macchi, G. Pedrolli, V. Tognetti, and R. Vaia, Phys. Rev. B **56**, 51 (1997).
[18] J.L. Barrat, P. Loubeyre, and M.L. Klein, J. Chem. Phys. **90**, 5644 (1989).
[19] M. Boninsegni, C. Pierleoni, and D.M. Ceperley, Phys. Rev. Lett. **72**, 1854 (1994).
[20] M.H. Müser, P. Nielaba, and K. Binder, Phys. Rev. B **51**, 2723 (1995).
[21] J.C. Noya, C.P. Herrero, and R. Ramírez, Phys. Rev. B **56**, 237 (1997).
[22] C.P. Herrero, Phys. Status Solidi B **220**, 857 (2000).
[23] R. Giachetti and V. Tognetti, Phys. Rev. B **33**, 7647 (1986).
[24] R.P. Feynman and H. Kleinert, Phys. Rev. A **34**, 5080 (1986).
[25] A. Cuccoli, A. Macchi, M. Neumann, V. Tognetti, and R. Vaia, Phys. Rev. B **45**, 2088 (1992).
[26] D. Acocella, G.K. Horton, and E.R. Cowley, Phys. Rev. B **61**, 8753 (2000).
[27] D. Acocella, G.K. Horton, and E.R. Cowley, Phys. Rev. Lett. **74**, 4887 (1995).
[28] D. Chandler and P.G. Wolynes, J. Chem. Phys. **74**, 4078 (1981).
[29] J.C. Noya, C.P. Herrero, and R. Ramírez, Phys. Rev. B **53**, 9869 (1996).
[30] M.J. Gillan, Philos. Mag. A **58**, 257 (1988).
[31] D.M. Ceperley, Rev. Mod. Phys. **67**, 279 (1995); **71**, S438 (1999).
[32] D. Thirumalai, R.W. Hall, and B.J. Berne, J. Chem. Phys. **81**, 2523 (1984).
[33] K. Singer and W. Smith, Mol. Phys. **64**, 1215 (1988).
[34] K. Binder and D.W. Heermann, *Monte Carlo Simulation in Statistical Physics* (Springer, Berlin, 1988).
[35] C.P. Herrero, J. Non-Cryst. Solids, **271**, 18 (2000).
[36] A. Cuccoli, A. Macchi, G. Pedrolli, V. Tognetti, and R. Vaia, Phys. Rev. B **51**, 12 369 (1995).
[37] These authors removed the ^{21}Ne and ^{22}Ne scattering contributions by modeling the scattering in the neutron time-of-flight spectrum.
[38] M. Berheide, W.H. Schulte, H.W. Becker, L. Borucki, M. Buschmann, N. Piel, C. Rolfs, G.E. Mitchell, and J.S. Schweitzer, Phys. Rev. B **58**, 11 103 (1998).
[39] H.T. Weston and W.B. Daniels, Phys. Rev. B **29**, 2709 (1984).
[40] H. Fenichel and B. Serin, Phys. Rev. **142**, 490 (1966).
[41] N.W. Ashcroft and N.D. Mermin, *Solid State Physics* (Saunders College, Philadelphia, 1976).
[42] D.N. Batchelder, D.L. Losee, and R.O. Simmons, Phys. Rev. **162**, 767 (1967).
[43] K.T. Tang and J.P. Toennis, J. Chem. Phys. **80**, 3726 (1984).
[44] C.P. Herrero and R. Ramírez, Phys. Rev. B **63**, 024103 (2001).
[45] A. Debernardi and M. Cardona, Phys. Rev. B **54**, 11 305 (1996).